

Projection deconvolution for proton CT using the spatially variant path uncertainty

Feriel Khellaf, Nils Krah, Jean Michel Létang and Simon Rit

Munich, October 13, 2022

CREATIS

Disclaimer

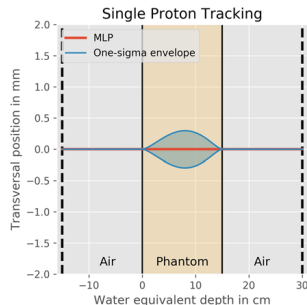
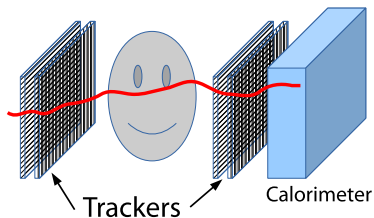
Follow up to Ferial's presentation at the Loma Linda workshop in 2020¹ based on her journal article².

¹F. Khellaf et al. "A deconvolution method to improve spatial resolution in proton CT". In: *The Sixth Loma Linda Workshop*. Loma Linda, USA, 2020.

²F. Khellaf et al. "Projection deconvolution for proton CT using the spatially variant path uncertainty". In: *IEEE Trans Radiat Plasma Med Sci* (2022). DOI: [10.1109/TRPMS.2022.3167334](https://doi.org/10.1109/TRPMS.2022.3167334).

Spatial resolution in ion CT

Limited by the stochastic curved path due to Coulomb scattering.



Even with pairs of ideal trackers before and after the scanned object, the spatial resolution will be limited by the uncertainty on the most likely path³.

³N. Krah et al. "A comprehensive theoretical comparison of proton imaging set-ups in terms of spatial resolution." In: *Phys Med Biol* 63.13 (13 2018), p. 135013. DOI: 10.1088/1361-6560/aacalf.

Resolution modeling

“Aims to model the very phenomena that degrade resolution within the reconstruction algorithm”⁴

Clinically used in emission tomography, has also been investigated in x-ray CT⁵

⁴A. Rahmim, J. Qi, and V. Sossi. “Resolution modeling in PET imaging: Theory, practice, benefits, and pitfalls”. In: *Med Phys* 40.6Part1 (2013), p. 064301. DOI: 10.1118/1.4800806.

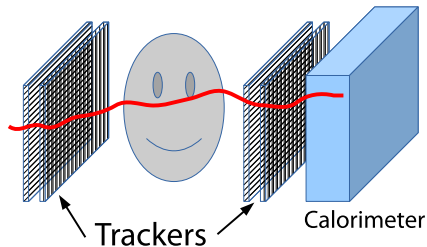
⁵S. Tilley II, J.H. Siewerdsen, and J.W. Stayman. “Model-based iterative reconstruction for flat-panel cone-beam CT with focal spot blur, detector blur, and correlated noise.”. In: *Phys Med Biol* 61.1 (2016), pp. 296–319. DOI: 10.1088/0031-9155/61/1/296.

Goal

Deconvolve the blur due to the path uncertainty in the distance-driven binning algorithm⁶.

⁶S. Rit et al. "Filtered backprojection proton CT reconstruction along most likely paths". In: *Med Phys* 40.3, 031103 (2013), p. 031103. DOI: [10.1118/1.4789589](https://doi.org/10.1118/1.4789589).

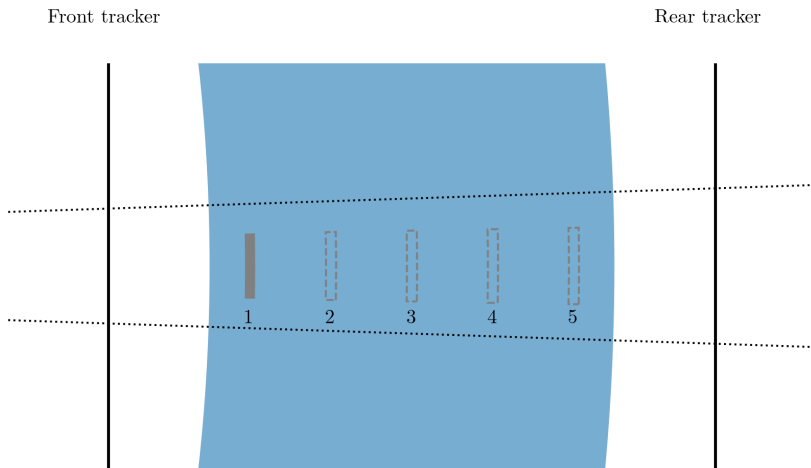
Simulated scanners with GATE



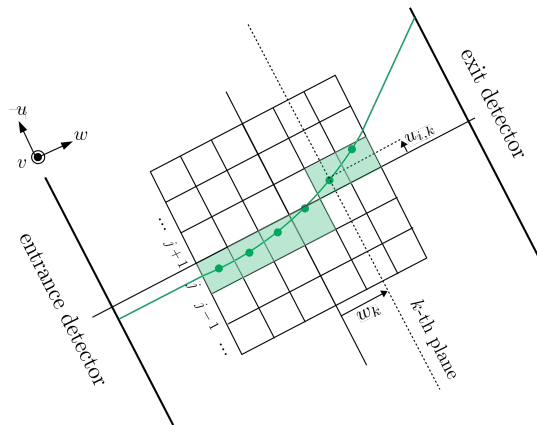
- 1 **Ideal trackers:** perfect measurements of the position and direction of the protons before and after the object
- 2 **Realistic trackers:** postprocessing of ideal data using
 - a strip pitch of 228 μm ,
 - a material budget of $x/X_0 = 5 \times 10^{-3}$,
 - a distance of 10 cm between the trackers,
 i.e. in usual specifications of pCT scanners⁷.

⁷V.A. Bashkirov et al. "Development of proton computed tomography detectors for applications in hadron therapy". In: *Nuclear Instruments and Methods in Physics Research Section A: Accelerators, Spectrometers, Detectors and Associated Equipment* 809 (2016), pp. 120–129. DOI: [10.1016/j.nima.2015.07.066](https://doi.org/10.1016/j.nima.2015.07.066).

Test object



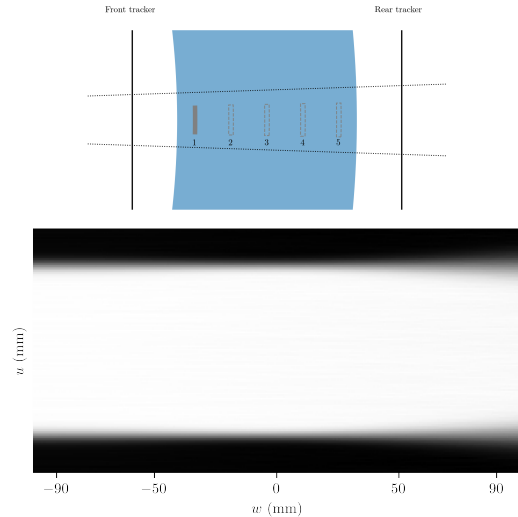
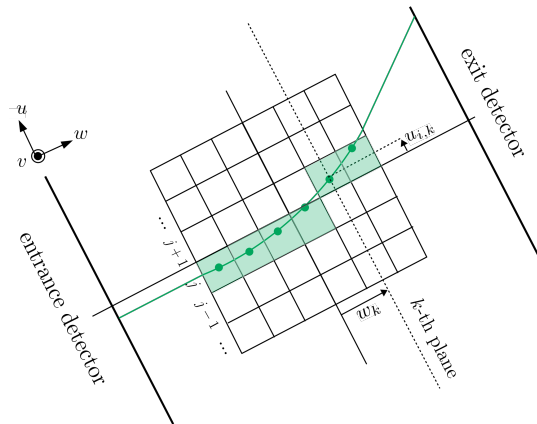
Distance-driven binning



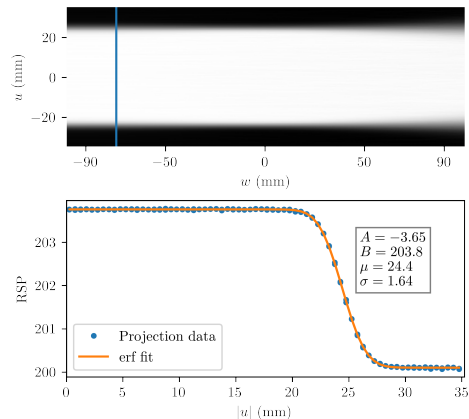
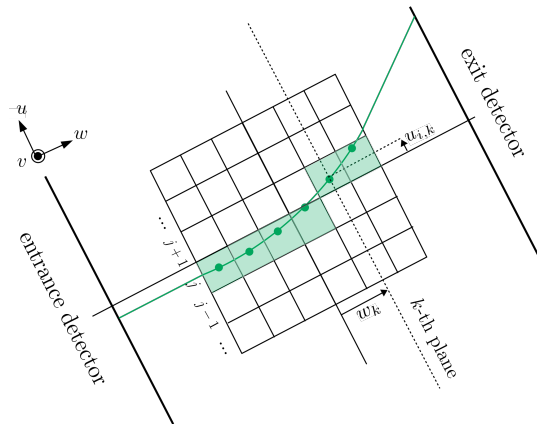
$$g_{j,k,p} = \frac{\sum_{i \in \mathbb{I}_p} \zeta_j(u_{i,k}, v_{i,k}, w_k) \text{WEPL}_i}{\sum_{i \in \mathbb{I}_p} \zeta_j(u_{i,k}, v_{i,k}, w_k)} \quad (1)$$

with \mathbb{I}_p the subset of protons for a given detector orientation and ζ_j the indicator function of the j -th pixel.

Distance-driven binning



Distance-driven binning



Blur model⁸

The likelihood that a proton passes through an intermediate position \mathbf{y}_1 and $\tilde{\mathbf{y}}_{\text{out}}$ given $\tilde{\mathbf{y}}_{\text{in}}$ is

$$L(\mathbf{y}_1, \tilde{\mathbf{y}}_{\text{out}} | \tilde{\mathbf{y}}_{\text{in}}) = \int L_{\text{scat}}(\mathbf{y}_1 | \mathbf{y}_{\text{in}}) L_{\text{meas}}(\tilde{\mathbf{y}}_{\text{in}} | \mathbf{y}_{\text{in}}) d\mathbf{y}_{\text{in}} \times \int L_{\text{scat}}(\mathbf{y}_{\text{out}} | \mathbf{y}_1) L_{\text{meas}}(\tilde{\mathbf{y}}_{\text{out}} | \mathbf{y}_{\text{out}}) d\mathbf{y}_{\text{out}} \quad (1)$$

⁸N. Krah et al. "A comprehensive theoretical comparison of proton imaging set-ups in terms of spatial resolution." In: *Phys Med Biol* 63.13 (13 2018), p. 135013. DOI: [10.1088/1361-6560/aacaf1](https://doi.org/10.1088/1361-6560/aacaf1).

Blur model⁸

The likelihood that a proton passes through an intermediate position \mathbf{y}_1 and $\tilde{\mathbf{y}}_{\text{out}}$ given $\tilde{\mathbf{y}}_{\text{in}}$ is

$$L(\mathbf{y}_1, \tilde{\mathbf{y}}_{\text{out}} | \tilde{\mathbf{y}}_{\text{in}}) = \int L_{\text{scat}}(\mathbf{y}_1 | \mathbf{y}_{\text{in}}) L_{\text{meas}}(\tilde{\mathbf{y}}_{\text{in}} | \mathbf{y}_{\text{in}}) d\mathbf{y}_{\text{in}} \quad (1)$$

$$\begin{aligned} & \times \int L_{\text{scat}}(\mathbf{y}_{\text{out}} | \mathbf{y}_1) L_{\text{meas}}(\tilde{\mathbf{y}}_{\text{out}} | \mathbf{y}_{\text{out}}) d\mathbf{y}_{\text{out}} \\ & \propto \exp\left(-\frac{1}{2}(\mathbf{y}_1 - \mathbf{y}_{\text{MLP}}(\mathbf{w}))^T \Sigma_{\text{MLP}}(\mathbf{w})^{-1} (\mathbf{y}_1 - \mathbf{y}_{\text{MLP}}(\mathbf{w}))\right) \quad (2) \end{aligned}$$

under the usual Gaussian approximation.

⁸N. Krah et al. "A comprehensive theoretical comparison of proton imaging set-ups in terms of spatial resolution." In: *Phys Med Biol* 63.13 (13 2018), p. 135013. DOI: 10.1088/1361-6560/aacaf.

Blur model⁸

The likelihood that a proton passes through an intermediate position \mathbf{y}_1 and $\tilde{\mathbf{y}}_{\text{out}}$ given $\tilde{\mathbf{y}}_{\text{in}}$ is

$$L(\mathbf{y}_1, \tilde{\mathbf{y}}_{\text{out}} | \tilde{\mathbf{y}}_{\text{in}}) = \int L_{\text{scat}}(\mathbf{y}_1 | \mathbf{y}_{\text{in}}) L_{\text{meas}}(\tilde{\mathbf{y}}_{\text{in}} | \mathbf{y}_{\text{in}}) d\mathbf{y}_{\text{in}} \quad (1)$$

$$\begin{aligned} & \times \int L_{\text{scat}}(\mathbf{y}_{\text{out}} | \mathbf{y}_1) L_{\text{meas}}(\tilde{\mathbf{y}}_{\text{out}} | \mathbf{y}_{\text{out}}) d\mathbf{y}_{\text{out}} \\ & \propto \exp\left(-\frac{1}{2}(\mathbf{y}_1 - \mathbf{y}_{\text{MLP}}(\mathbf{w}))^T \Sigma_{\text{MLP}}(\mathbf{w})^{-1} (\mathbf{y}_1 - \mathbf{y}_{\text{MLP}}(\mathbf{w}))\right) \quad (2) \end{aligned}$$

under the usual Gaussian approximation.

$\mathbf{y}_{\text{MLP}}(\mathbf{w})_1$ is the most likely position,

$\Sigma_{\text{MLP}}(\mathbf{w})_{1,1}$ is the squared path uncertainty $\sigma_{\text{MLP}}(\mathbf{w})^2$

⁸N. Krah et al. "A comprehensive theoretical comparison of proton imaging set-ups in terms of spatial resolution." In: *Phys Med Biol* 63.13 (13 2018), p. 135013. DOI: 10.1088/1361-6560/aacaf1.

Shift-variant blur

Distance-driven binning of the path uncertainty

$$\sigma_{j,k,p} = \sqrt{\frac{\sum_{i \in \mathbb{I}_p} \zeta_j(\mathbf{u}_{i,k}, \mathbf{v}_{i,k}, \mathbf{w}_k) \sigma_{\text{MLP},i}^2(\mathbf{w}_k)}{\sum_{i \in \mathbb{I}_p} \zeta_j(\mathbf{u}_{i,k}, \mathbf{v}_{i,k}, \mathbf{w}_k)}} \quad (3)$$

The projection g resulting from the distance-driven binning is the result of a shift-variant blur of the non-blurred projection g^*

$$\mathbf{g}_{k,p} = \mathbf{H}_{k,p} \mathbf{g}_{k,p}^* \quad (4)$$

where $h_{j-m,m,k,p}$ is computed from a 1D Gaussian function due to the Gaussian model used for the MLP uncertainty

$$h_{j-m,m,k,p} = \frac{1}{\sqrt{2\pi}\sigma_{m,k,p}} \exp\left(-\frac{(j-m)^2\tau^2}{2\sigma_{m,k,p}^2}\right) \quad (5)$$

One-dimensional deconvolution

The problem

$$\hat{\mathbf{g}}_{k,p} = \arg \min_{\mathbf{g}_{k,p}^*} \|\mathbf{H}_{k,p}^\beta \mathbf{g}_{k,p}^* - \mathbf{g}_{k,p}\|_2^2 + \alpha^2 \|\nabla \mathbf{g}_{k,p}^*\|_2^2 \quad (6)$$

was solved with a conjugate gradient method. It has two hyper-parameters:

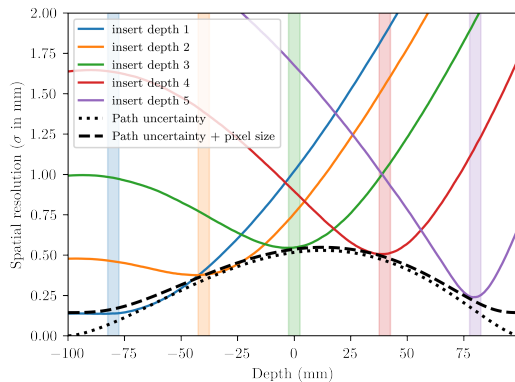
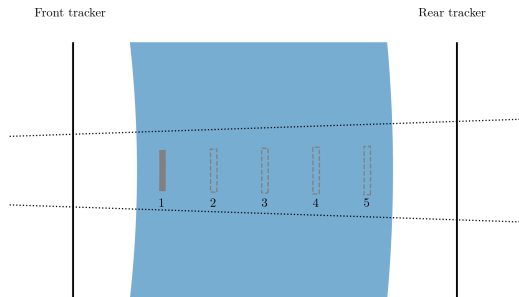
- α controls the spatial regularization⁹,
- $\beta \in (0, 1]$ is an underestimation of the uncertainty to reduce overshoot artifacts^{10,11}.

⁹J. Nuyts. "Unconstrained image reconstruction with resolution modelling does not have a unique solution". In: *EJNMMI Physics* 1.1 (2014), p. 98. DOI: 10.1186/s40658-014-0098-4.

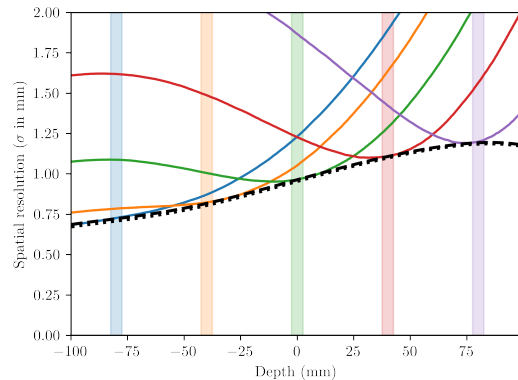
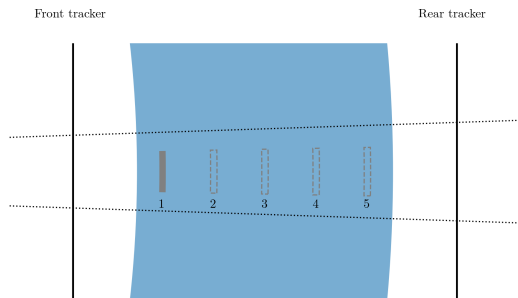
¹⁰S. Tong et al. "Properties and mitigation of edge artifacts in PSF-based PET reconstruction". In: 58.5 (2011), pp. 2264–2275. DOI: 10.1109/TNS.2011.2164579.

¹¹S. Stute and C. Comtat. "Practical considerations for image-based PSF and blobs reconstruction in PET". In: *Phys Med Biol* 58 (11 2013), pp. 3849–3870. DOI: 10.1088/0031-9155/58/11/3849.

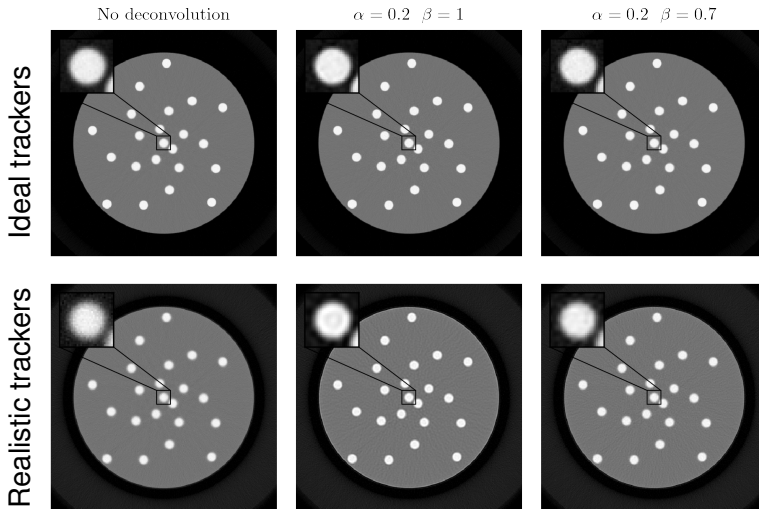
Blur model - Ideal trackers



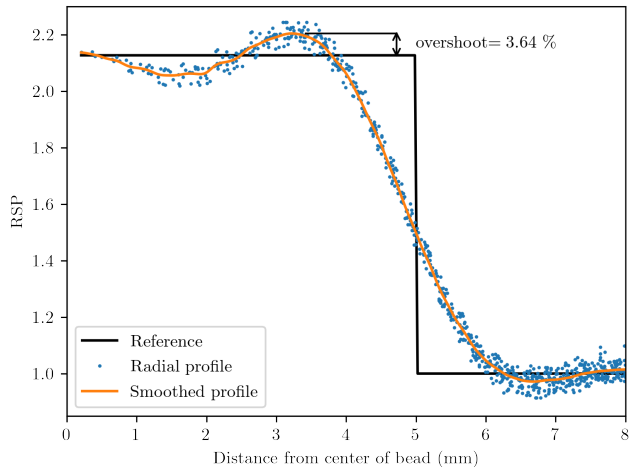
Blur model - Realistic trackers



Resolution phantom

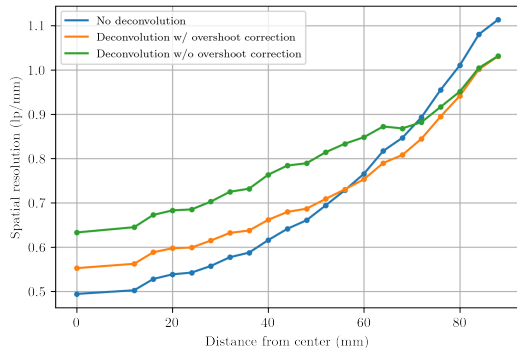


Overshoot artifacts

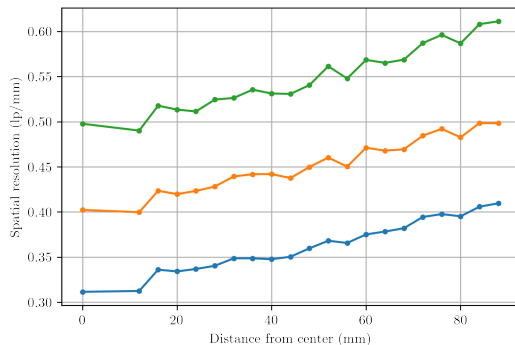


Resolution phantom

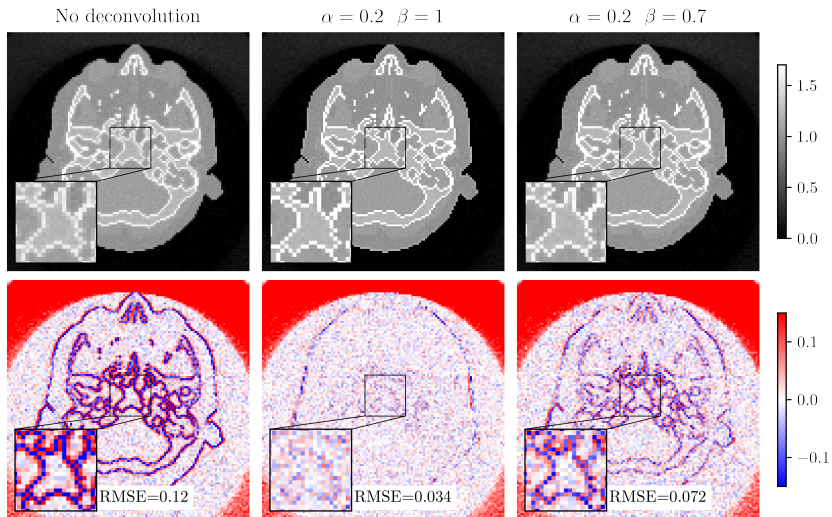
Ideal trackers



Realistic trackers



ICRP phantom - Head

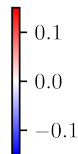
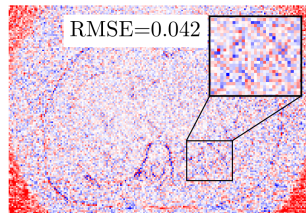
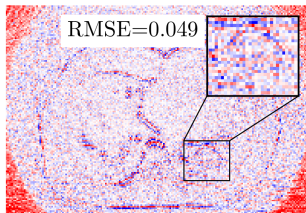
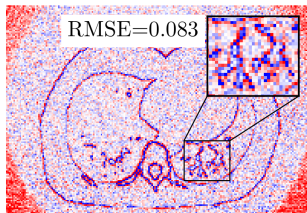
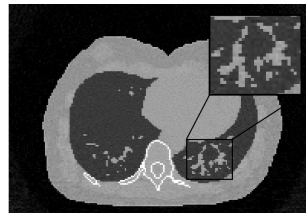
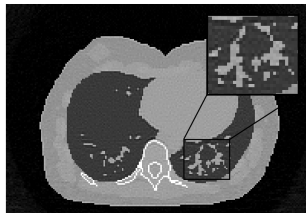
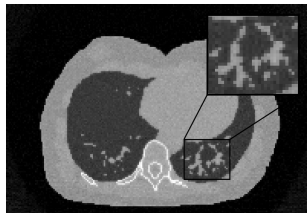


ICRP phantom - Lungs

No deconvolution

$\alpha = 0.2 \quad \beta = 1$

$\alpha = 0.2 \quad \beta = 0.7$



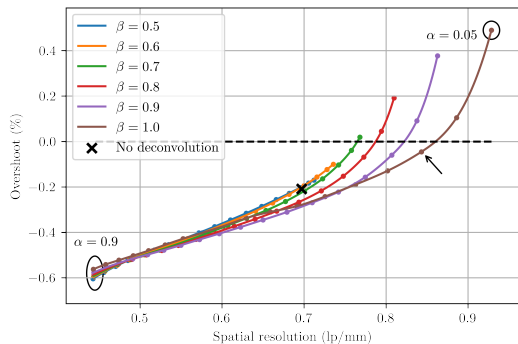
Conclusions

- Blur in binned projections due to MCS can be modeled under a Gaussian approximation.
- Proof-of-concept 1D deconvolution of projections obtained with distance-driven binning with spatial regularization and correction of overshoot artifacts.
- Resolution modeling has the potential to improve spatial resolution.
 - Up to 29% without introducing overshoot artifacts in the resolution phantom.
 - Visual enhancement of spatial resolution in anthropomorphic images which had less overshoot artifacts.
- Potential improvements with alternative approaches (2D/3D deconvolution, iterative reconstruction¹², etc.)

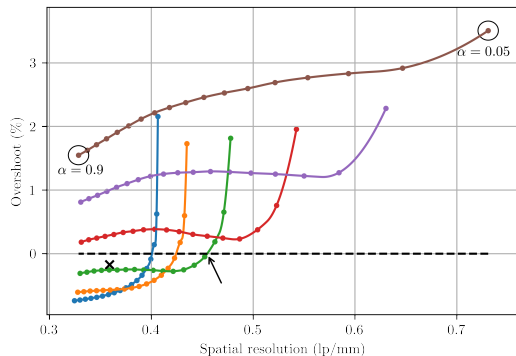
¹²D. Wang, T.R. Mackie, and W.A. Tomé. "On the use of a proton path probability map for proton computed tomography reconstruction". In: *Med Phys* 37.8 (2010), pp. 4138–4145.

Tuning of the hyperparameters

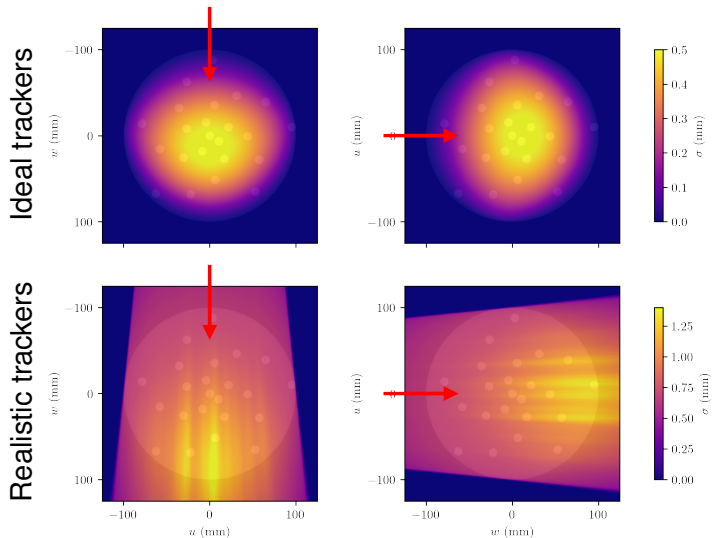
Ideal trackers



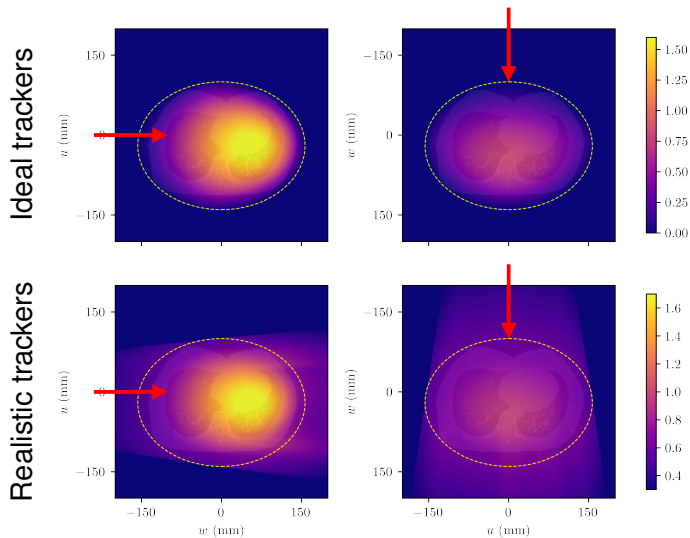
Realistic trackers



Uncertainty maps



Uncertainty maps



Uncertainty maps

